Preparation of Ordered Mesoporous SiC from Preceramic Polymer Templated by Nanoporous Silica

Jia Yan,[†,‡] Anjie Wang,[†] and Dong-Pyo Kim*,[§]

State Key Laboratory of Fine Chemicals, Dalian University of Technology, 158 Zhongshan Road, Dalian 116012, P. R. China, and Department of Fine Chemical Engineering and Chemistry, Chungnam National University, Daejeon 305-764, Korea

Highly ordered mesoporous SiC materials were prepared by infiltrating viscous liquid preceramic polymer, allylhydridopolycarbosilane, into two types of surface modified nanoporous silica templates: mesoporous silica SBA-15 and mesocellular siliceous foam. The silica templates were subsequently etched off after pyrolysis at 1000 °C under nitrogen atmosphere with the resultant formation of ordered mesoporous structures. The mesoporous SiC materials, synthesized from both types of templates possessed high Brunauer−Emmett−Teller (BET) surface areas in the range of 250−260 m^2/g with pore sizes of 3.4−3.6 nm. The ordered structures of mesoporous SiC were exact inverse replicas of their respective silica templates, as characterized by small angle X-ray diffraction (XRD), transmission electron microscope (TEM) images, and the adsorption−desorption isotherm of nitrogen.

Introduction

Silicon carbide (SiC) is known to possess unique properties such as high thermal conductivity, excellent thermal stability, resistance toward oxidation, high mechanical strength, and chemical inertness. These properties make SiC a suitable material for various applications such as catalyst support,[1] in the design of high-temperature semiconducting devices,[2] and as metal or polymer matrix composites.[3] Especially, because of the low oxidation resistance of carbon and poor hydrothermal stability of silica porous materials, SiC with a high surface area has been widely used as a catalyst support material at high temperatures in the catalysis field.[4] Therefore, there have been various attempts to prepare SiC materials with high surface areas.[5,6] Recently, the sacrificial template method has been widely used for the synthesis of various tailored SiC nanostructures. For example, SiC nanotubes were obtained from an alumina membrane template,[7] SiC-based ceramic hollow sphere assemblies were prepared using macroporous carbon as a template,[8] and macroporous SiC was synthesized from a silica sphere template.[9] In the field of mesoporous materials, some mesoporous SiC materials were prepared via a carbothermal reduction reaction by employing mesoporous silica MCM-48 as a template[10] or by shape memory synthesis in an active charcoal template.[1] Krawiec et al. successfully achieved the formation of disordered amorphous mesoporous SiC with a high surface area (508 m^2/g) by chemical vapor infiltration (CVI) of gaseous precursor into a mesoporous SBA-15 template.[11] However, to date, the synthetic approaches for ordered mesoporous SiC with monodisperse pores have not been reported, although only a few mesoporous SiC materials with no ordered pore structure have been demonstrated.

In our present paper, we report the synthesis of ordered mesoporous SiC materials by using two types of nanoporous silica as templates (SBA-15 and mesocellular siliceous foam), and a low viscosity liquid polymer allylhydridopolycarbosilane as a stoichiometric SiC precursor. SBA-15 is a two-dimensional hexagonally ordered mesoporous silica material with channel-interconnecting micropores within the wall, which can be prepared by employing triblock copolymer, $EO_{20}PO_{70}EO_{20}$, as a structure directing agent.[12] Mesocellular siliceous foam (MCF), which is composed of uniform and large spherical cells (∼20 nm) and connecting windows, is the product of the phase transformation from the ordered *p6mm* mesostructure of SBA-15-type mesoporous silica induced by an organic cosolvent, trimethylbenzene.[13] Similar to the case of mesoporous carbon CMK-3 which is an inverse replica of its template (SBA-15),[14] this work is the first example to demonstrate the synthesis of ordered mesoporous SiC, which retains the structural symmetry of its silica template.

Experimental Section

Synthesis and Modification of Nanoporous Silica Templates. (1) Synthesis of SBA-15. High-quality SBA-15 samples were prepared by employing the triblock copolymer, $EO_{20}PO_{70}$-EO_{20} (Pluronic P123, Aldrich), as the surfactant and tetraethyl orthosilicate (TEOS, 98%, Aldrich) as the silica source, as reported by Zhao et al.[12] The starting composition was in the following ratio: 4 g of P123:0.041 mol TEOS:0.24 mol HCl: 6.67 mol H_2O. Typically, 8.5 g of TEOS was added to 150 mL of 1.6 M HCl containing 4 g of P123 at 35 °C. After stirring for 5 min, the mixture was placed in an oven at 35 °C for 24 h and, subsequently, at 100 °C for 48 h. The product was filtered, dried without washing, and calcined in air at 550 °C for 6 h.

(2) Synthesis of Mesocellular Siliceous Foam (MCF). To prepare MCF, 1,3,5-trimethylbenzene (TMB, 98%, Aldrich) as a swelling agent was added with a TMB/P123 weight ratio of 3:4.[12,13] The overall synthetic procedure was very similar to that applied for the synthesis of the above-mentioned SBA-15.

* Corresponding author's e-mail: dpkim@cnu.ac.kr. Tel.: 82-42-821-7684. Fax: 82-42-823-6665.
† Dalian University of Technology.
‡ Jia Yan worked at Prof. Kim's lab under a co-advisor program.
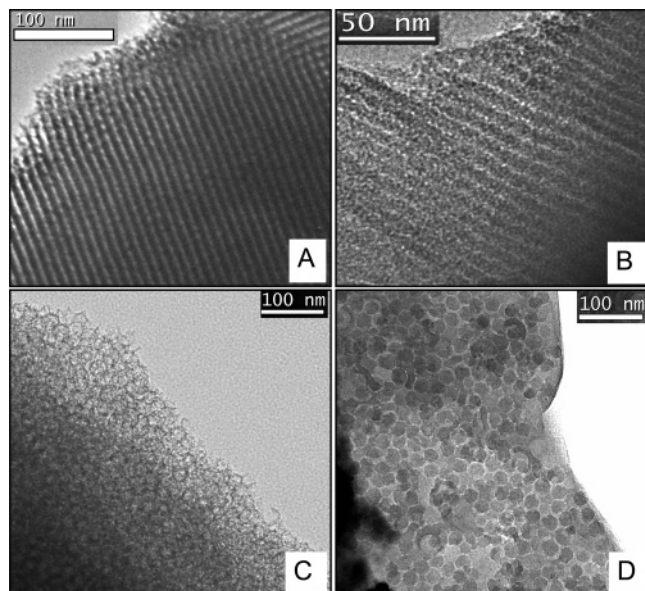§ Chungnam National University.

(3) Modification of Both of the Silica Templates. For the efficient infiltration of organic precursor, the hydrophilic channel surface of both the silica templates was modified into a hydrophobic surface by introducing trimethylsilyl, as reported by Beck et al.[15] In a typical experiment, 0.5 g of silica template, 10 g of $(CH_3)_3SiCl$ (TMSCl, Aldrich), and 15 g of $((CH_3)_3\text{-}Si)_2O$ (HMDS, Aldrich) were refluxed overnight with magnetic stirring under nitrogen atmosphere. The volatiles were stripped on a rotary evaporator, and the dry powder was washed two or three times with 10 mL of acetone by centrifugation.

Synthesis of Mesoporous SiC from Surface Modified Silica Templates. The allylhydridopolycarbosilane (AHPCS, SMP-10, Starfire Systems, Inc.), with a viscosity of 45−120 cP and density of 0.998 g/cm^3 as a stoichiometric SiC precursor, was diluted in tetrahydrofuran (THF, Aldrich) to form 15 and 30 wt % solutions. The chemical formula of AHPCS is as follows:

A 0.1 g portion of modified MCF template was immersed in 30 wt % of the polymeric solution under nitrogen atmosphere at room temperature for 48 h. By measuring the weight increase, 0.35 g of polymer solution was infiltrated into the template. The infiltrated template was dried and cured at 180 °C for 24 h under vacuum. The cured polymer−silica composite was re-infiltrated with 15 wt % polymer solution, resulting in 0.30 g of weight gain. It was subsequently dried and cured by a similar procedure as discussed above. The sample was heated to 1000 °C under nitrogen atmosphere at a heating rate of 1 °C/min to convert the polymer to the SiC phase. The silica frameworks were dissolved by using a 10 wt % HF solution in a 50:50 mixture of water and ethanol. The resulting porous SiC was repeatedly washed with distilled water and dried at 150 °C for 6 h. Alternatively, for the modified SBA-15 template, the identical procedure mentioned above was followed. Subsequently, the respective weight gains of 0.30 and 0.25 g by the diluted polymeric solutions were observed after the first and second infiltration step. The template-free mesoporous SiC products from SBA-15 and MCF were designated as MSiC-SBA and MSiC-MCF, respectively.

Characterization of Silica Templates and Mesoporous SiC Products. Small-angle X-ray diffraction (XRD) patterns were recorded on an MX Labo powder diffractometer equipped with CuKα radiation (40 kV, 20 mA) at the rate of 1.0°/min over the range of 0.2−6.0° (2θ). High-resolution transmission electron microscope (HRTEM) images were taken at 200 kV (JEM 2100F, JEOL, Japan). The Brunauer−Emmett−Teller (BET) surface area and N_2 adsorption−desorption isotherms were measured at 77K on an ASAP 2010 analyzer (Micromeritics). The chemical structure of materials was investigated by ^{29}Si magic-angle spinning (MAS) NMR spectra which were performed on an FT Wide Bore (600 MHz) Unityl NOVA600 under cross polarization magic-angle spinning (CPMAS) conditions. X-ray photoelectron spectra (XPS) analysis was carried out using an ESCA 2000 XPS with an MgKα X-ray source.

Results and Discussion

Small-angle X-ray diffraction (SA-XRD) patterns of the SBA-15 template, MSiC-SBA/silica composite, and template-free

Figure 1. Small-angle XRD patterns of (a line 1) MSiC-SBA, (a line 2) SBA-15 template, (a line 3) SiC-SBA/silica composite, (b line 1) MSiC-MCF, (b line 2) MCF template, and (b line 3) MSiC-MCF/silica composite.

MSiC-SBA are presented in Figure 1a. In the XRD pattern of SBA-15 (Figure 1a line 2), a major peak at $2\theta = 0.94°$ and two minor peaks at 1.63° and 1.87° can be assigned to (100), (110), and (200) diffractions of the 2-D hexagonal space group ($p6mm$), which is in agreement with the previous work.[12] The intense (100) peak reflects a d spacing of 9.41 nm, corresponding to a unit cell parameter a_0 of 10.9 nm. In the case of MSiC-SBA/silica composite (Figure 1a line 3), no diffraction peaks were observed. The absence of diffraction peaks could be due to complete pore filling of the SBA-15 template by the SiC phase. However, once the silica template was removed for SiC sample (Figure 1a line 1), a broad diffraction peak was recovered at $2\theta = 1.22°$, corresponding to a d spacing of 7.24 nm. The corresponding a_0 value was 8.36 nm, which was 2.54 nm smaller than that of the SBA-15 template, due to structural shrinkage during the pyrolysis process.[14]

Figure 1b represents the typical SA-XRD patterns of the MCF template, MSiC-MCF/silica composite, and template-free MSiC-MCF. The XRD pattern of MCF (Figure 1b line 2) shows four peaks with d spacings of 22.34, 13.17, 9.24, and 7.0 nm at very low angles (2θ range from 0.3−1°), as is consistent with the previous reports.[12,13] As analyzed by Schmidt-Winkel et al.,[13] though these peaks cannot be indexed to any plane or space group (e.g., $p6mm$), they indicate that MCF is composed of monodisperse cells with uniform size. In the case of MSiC-MCF/silica composite (Figure 1b line 3), the diffraction peaks disappeared due to complete pore filling of the MCF template. After the removal of the silica template to attain the final SiC sample (Figure 1b line 1), four well-resolved diffraction peaks with d spacings of 19.4, 11.7, 8.2, and 5.7 nm were observed at low angles, similar to the case of MCF, except for a little reduction in the d spacing, which was due to microstructural shrinkage during the pyrolysis step.[14] Upon comparison with MSiC-SBA (Figure 1a line 1), the SA-XRD pattern of MSiC-MCF (Figure 1b line 1) was more similar to that of its silica template. It was probably because the larger pores of the MCF template were much easier to be infiltrated by the viscous preceramic polymer.

At this point, it is worth mentioning that, as reported previously, none of the mesoporous SiC materials, including ones prepared by carbothermal reduction[10] or the CVI[11] method, showed long range order of the channels in small-angle X-ray diffraction. On the contrary, the presence of long range order of channels was a remarkable feature in our study. In addition, the internal pore surface of silica templates was necessarily modified into a hydrophobic surface via trimethylsilylation. The

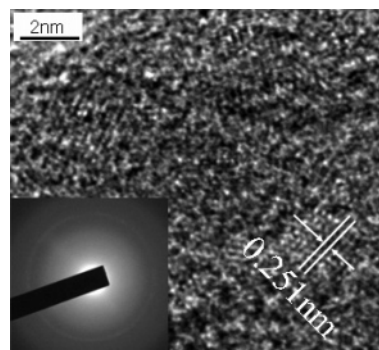**Figure 2.** TEM images of (A) SBA-15, (B) MSiC-SBA, (C) MCF, and (D) MSiC-MCF.

Figure 3. HRTEM image of an SiC wall of MSiC-MCF. A selected area electron diffraction pattern is shown inset.

Figure 4. ^{29}Si MAS NMR spectra of MSiC-MCF.

mentioned afore step was carried out under the notation that the hydrophobic AHPCS preceramic polymer readily wets the inner surface of modified silica template, rather than the hydrophilic unmodified surface.[16] It is also imperative to understand that the hydrophilic Si−OH or strongly adsorbed moisture on the unmodified surface of the silica template might attack and decompose the precursor due to the chemical sensitivity of the infiltrated preceramic polymer.[16]

Figure 2 shows TEM images of the silica templates and template-free mesoporous SiC products, which reveal that, like mesoporous carbon CMK-3, the structures of the mesoporous SiC samples were exact inverse replicas of their silica templates with highly ordered microstructures. Since the dry pores of both the templates were effectively filled with the polymer, followed by a subsequent series of curing, pyrolysis and etching step, it turned out that the obtained mesoporous SiC products retained the structural symmetry of silica templates. The void channels of SBA-15 template (Figure 2A) were converted into the SiC ceramic walls (Figure 2B), whereas the silica walls of SBA-15 were removed to form hollow channels of MSiC-SBA. In the alternative case of MSiC-MCF, the ∼20 nm hollow pores of the MCF template (Figure 2C) were completely filled by the precursor to form a SiC ceramic wall of ∼18 nm in diameter (Figure 2D), while the walls of the silica template were transformed into hollow pores. In this case, it was generally observed that most of the different sized pores of the templates were converted into the dense walls of mesoporous SiC materials with the corresponding dimension; however, a silica solid network with slightly different wall thickness produced the nearly identical pore size of mesoporous SiC.

On the other hand, the high-resolution TEM image of the template-free MSiC-MCF sample in Figure 3 displays nanoscale crystalline domains in the amorphous matrix with a lattice *d* spacing of 0.251 nm, indicating the SiC crystalline structure as reported in the literature.[17] It was also confirmed that selected area electron diffraction revealed the presence of a broad diffused ring indexed to the (111) plane, indicating the formation of a SiC phase.

Furthermore, in the ^{29}Si MAS NMR spectra (Figure 4) of the obtained mesoporous samples, the broad signal was centered at −8 ppm and covered a range between −30 and 10 ppm,
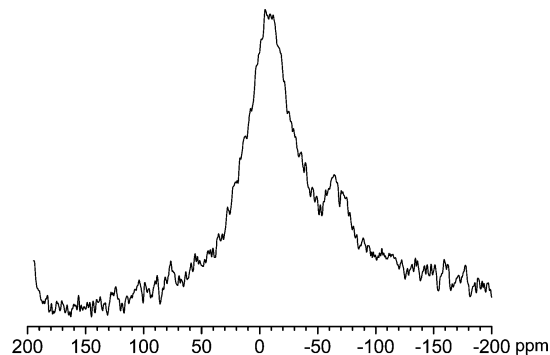
which is typical for amorphous SiC. The data were also consistent with the bulk conversion chemistry from AHPCS polymer to stoichiometric SiC at various temperatures up to 1400 °C.[18] In addition, a small peak centered at −62 ppm indicated the formation of $SiCO_3$ and SiC_2O_2 species.[11] However, the ratio of the integral area for SiC/SiC_xO_y was 5, indicating that SiC was a dominating phase in the mesoporous products. No peak was observed at −110 ppm, which indicated that SiO_2 templates were removed completely. Moreover, the Si 2p X-ray photoelectron spectra (XPS) gave similar results with a main peak at 100.2 eV (SiC, 82 at. %) and small portions of the peak at 102.2 eV (SiC_xO_y, 18 at. %).[11] The formation of SiO_xC_y phase was presumably caused by the interfacial diffusion of oxygen from the silica template into the SiC phase fully filling the channels of the template during the pyrolysis process at 1000 °C, and the process becomes drastically significant at higher temperatures. It was confirmed that the walls of the obtained mesoporous SiC materials should be a mixture of amorphous SiC and SiO_xC_y phase embedded with some nanoscale crystalline SiC phase.

Figure 5 shows the N_2 adsorption−desorption isotherms and the pore size distribution curves of silica templates and template-free SiC products. For both the silica templates (Figure 5A and B), the isotherms were of type IV with a hysteresis loop at a relative pressure of about 0.65, which was in agreement with previous work.[12] The porous SiC products exhibited similar types of isotherms with a hysteresis loop (Figure 5C and D), implying that both the products also possess mesoporous structure. The pore size distribution data determined by Barret−Joyner−Halenda (BJH) analysis indicated that both of the MSiC-SBA and MSiC-MCF materials were mostly mesoporous with quite narrow size distributions centered at 3.4 and 3.6 nm, respectively.

Table 1 summarizes the pore characteristics of the silica templates and template-free SiC products, as measured by N_2 adsorption−desorption experiments. The pore size and wall
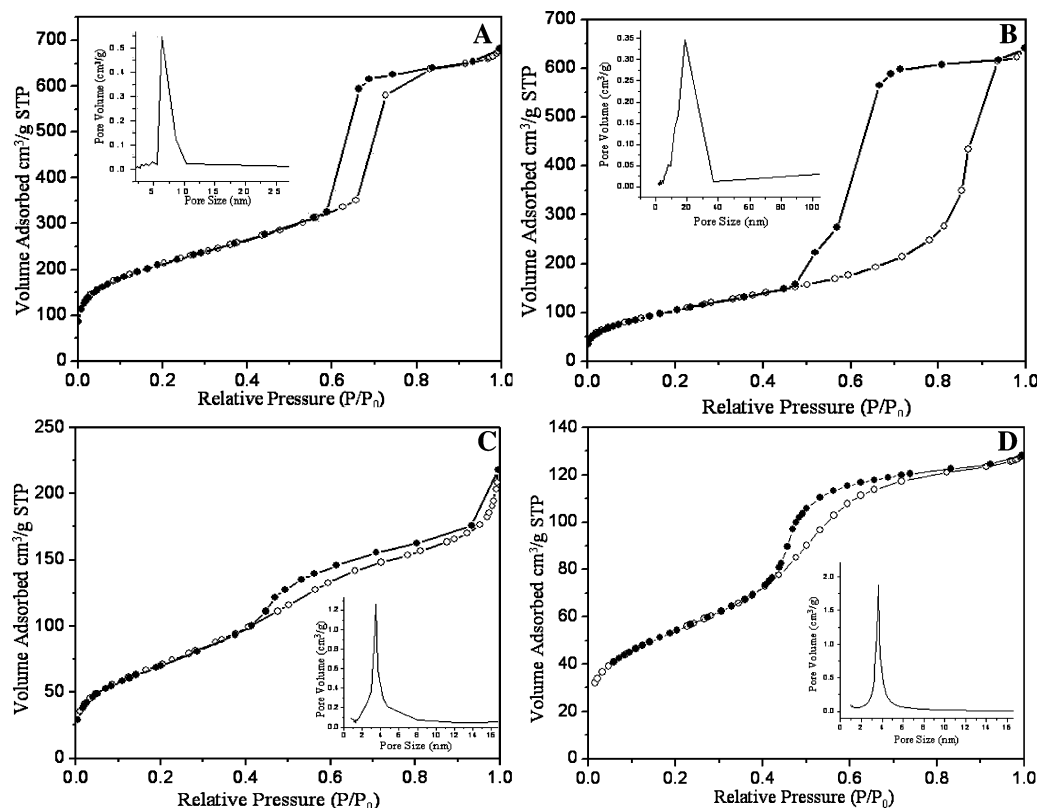
Figure 5. Nitrogen adsorption−desorption (○ and ●, respecitvely) isotherms of (A) the SBA-15 template, (B) the MCF template, (C) MSiC-SBA, and (D) MSiC-MCF at 77 K. The pore size distribution curves are shown inset.

TABLE 1: Textural Properties of SBA-15 and MCF Silica Templates and the Corresponding Mesoporous SiC Products

sample	$d_{(100)}$ (nm)	surface area[a] (m²/g)	pore size (nm)	pore volume[b] (cm³/g)	mesopore volume[c] (cm³/g)	wall thickness[d] (nm)
SBA-15	9.41	561	6.5	0.81	0.74	4.4
MSiC-SBA	7.24	260	3.4	0.34	0.29	4.96
MCF	22.34	389	20	0.99	0.95	5.8
MSiC-MCF	19.4	248	3.6	0.30	0.28	18.8

[a] Specific surface area according to Brunauer−Emmett−Teller (BET). [b] Total pore volume at $P/P_0 = 0.99$. [c] Calculated according to Barret-Joyner-Halenda (BJH) analysis (adsorption branch between 1.7 and 300 nm diameter). [d] The wall thicknesses were calculated by a_0 − pore size ($a_0 = 2d_{(100)}/3^{1/2}$).

thickness of mesoporous SiC products were consistent with the results obtained from SA-XRD and TEM measurements. For example, in the case of MSiC-SBA, the distance connecting two neighboring mesopores (a_0 parameter) was calculated to be 8.36 nm from SA-XRD results. Therefore, the difference between a_0 and the pore diameter (3.4 nm) corresponded to a wall thickness of 4.96 nm of the mesoporous SiC, which is in good agreement with the wall thickness observed in the TEM pictures. However, the 4.96-nm wall thickness was approximately 1.5 nm smaller than the pore diameter (6.5 nm) of its template, SBA-15. This slight numerical discrepancy between the corresponding templates and products can be assigned to the structural shrinkage occurring during the pyrolysis step, and similar behavior was also observed in the preparation of mesoporous carbon CMK-3 from a silica template.[14] On the other hand, the BET surface area and mesopore volume were 260 m²/g and 0.29 cm³/g for the MSiC-SBA sample and 248 m²/g and 0.28 cm³/g for the MSiC-MCF sample, which were relatively high when compared with the porous SiC produced by other methods. However, the significantly lower surface area than CMK-3 (∼1520 m²/g) could be due to the fact that carbon materials contain large parts of micropores and secondary mesopores, which contribute to the major part of the surface

area and pore volume.[14] In addition, compared with the very similar work recently reported by Shi et al.,[19] the lower surface area of the stoichiometric SiC product in our work was attributed to the presence of no residual carbon.

Conclusions

Highly ordered mesoporous SiC materials with high surface area have been prepared by using liquid preceramic polymer as a precursor and trimethylsilylated SBA-15 and MCF nanoporous silica as templates. The prepared mesoporous SiC materials from two types of silica templates were exact inverse replicas of their templates. It is expected that this novel technique can be suitable for the synthesis of many other types of ordered, mesoporous nonoxide ceramic materials with interesting pore topologies. These ordered mesoporous ceramics would hold imperative applications in the field of catalysis and membrane research being conducted at harsh conditions, where the metal and plastic materials and even oxide ceramics will not be applicable.

Preparation of Ordered Mesoporous SiC

J. Phys. Chem. B, Vol. 110, No. 11, 2006 **5433**

References and Notes

(1) Pham-Huu, C.; Bouchy, C.; Dintzer, T.; Ehret, G.; Estournes, C.; Ledoux, M. J. *J. Appl. Catal. A* **1999**, *180*, 385.

(2) Feng, Z. C.; Mascarenhas, A. J.; Choyke, W. J.; Powell, J. A. *J. Appl. Phys.* **1988**, *64*, 3176.

(3) Frevel, L. K.; Saha, C. K.; Petersen, D. R. *J. Mater. Sci.* **1995**, *30*, 3734.

(4) Ledoux, M. J.; Pham-Huu, C.; Chianelli, R. R.; Opin, C. *Solid State Mater. Sci.* **1996**, *1*, 96.

(5) Jin, G. Q.; Guo, X. Y. *Microporous Mesoporous Mater.* **2003**, *60*, 207.

(6) Pol, V. G.; Pol, S. V.; Gedanken, A. *Chem. Mater.* **2005**, *17*, 1797.

(7) Wang, H.; Li, X. D.; Kim, T. S.; Kim, D. P. *Appl. Phys. Lett.* **2005**, *86*, 173104.

(8) Wang, H.; Yu, J. S.; Li, X. D.; Kim, D. P. *Chem. Commun.* **2004**, 2352.

(9) Sung, I. K.; Yoon, S. B.; Yu, J. S.; Kim, D. P. *Chem. Commun.* **2002**, 1480.

(10) Parmentier, J.; Patarin, J.; Dentzer, J.; Vix-Guterl, C. *Ceram. Int.* **2002**, *28*, 1.

(11) Krawiec, P.; Weidenthaler, C.; Kaskel, S. *Chem. Mater.* **2004**, *16*, 2869.

(12) Zhao, D. Y.; Feng, J. L.; Huo, Q. S.; Melosh, N.; Fredrickson, G. H.; Chmelka, B. F.; Stucky, G. D. *Science* **1998**, *279*, 548.

(13) Schmidt-Winkel, P.; Lukens, W. W., Jr.; Zhao, D. Y.; Yang, P. D.; Chmelka, B. F.; Stucky, G. D. *J. Am. Chem. Soc.* **1999**, *121*, 254.

(14) Jun, S.; Joo, S. H.; Ryoo, R.; Kruk, M.; Jaroniec, M.; Liu, Z.; Ohsuma, T.; Terasaki, O. *J. Am. Chem. Soc.* **2000**, *122*, 10712.

(15) Beck, J. S.; Vartuli, J. C.; Roth, W. J.; Leonowicz, M. E.; Kresge, C. T.; Schmitt, K. D.; Chu, C. T.-W.; Olson, D. H.; Sheppard, E. W.; McCullen, S. B.; Higgins, J. B.; Schlenker, J. L. *J. Am. Chem. Soc.* **1992**, *114*, 10834.

(16) Yoon, S. B.; Kim, J. Y.; Yu, J. S. *Chem. Commun.* **2001**, 559.

(17) Pol, V. G.; Pol, S. V.; Gedanken, A. *Chem. Mater.* **2005**, *17*, 1797.

(18) Sung, I. K.; Mitchell, C. M.; Kim, D. P.; Kenis, P. J. A. *Adv. Funct. Mater.* **2005**, *15*, 1336.

(19) Shi, Y. F.; Meng, Y.; Chen, D. H.; Cheng, S. J.; Chen, P.; Yang, H. F.; Wan, Y.; Zhao, D. Y. *Adv. Funct. Mater.*, published online Jan 3, http://dx.doi.org/10.1002/adfm.200500643.